Low Temperature Physics/Fizika Nizkikh Temperatur, 2015, v. 41, No. 10, pp. 989–996

Effective magnetization damping for a dynamical spin texture in metallic ferromagnet

Oksana V. Sukhostavets[1], Julian M. Gonzalez[1], and Konstantin Y. Guslienko[1,2]

[1]*Dpto. Física de Materiales, Facultad de Química, Universidad del País Vasco, UPV/EHU*
20018 San Sebastián, Spain
E-mail: oksana.sukhostavets@ehu.eus

[2]*IKERBASQUE, The Basque Foundation for Science, 48013 Bilbao, Spain*

Received April 4, 2015, published online August 25, 2015

An additional magnetization damping for an inhomogeneous spin texture in metallic ferromagnets is calculated on the basis of the *s–d* exchange model. The effect of conduction electrons on the magnetization dynamics is accounted for the case of slowly varying spin texture within adiabatic approximation by using a coordinate transformation to the local quantization axis. The moving magnetic vortex in a circular nanodot made of permalloy is considered as an example. The dependence of the damping on the dot geometrical sizes is obtained. It is found that the additional damping can reach up to 50% of magnitude of the phenomenological Gilbert damping in the Landau–Lifshitz equation of magnetization motion and should be taken into account for any inhomogeneous spin texture dynamics in ferromagnetic metals.

PACS: 76.60.Es Relaxation effects;
76.20.+q General theory of resonances and relaxations;
75.75.–c Magnetic properties of nanostructures;
75.78.–n Magnetization dynamics.

Keywords: magnetization damping, magnetic vortex, ferromagnetic nanodot.

1. Introduction

The Landau–Lifshitz (LL) equation of motion was first introduced in 1935 as a phenomenological equation to describe the dynamics of magnetization field $\mathbf{M}(\mathbf{r})$ in a ferromagnet well below the Curie temperature [1], when the exchange energy dominates and the magnetization vector keeps its magnitude unchanged. If there is an effective field $\mathbf{H}_{\text{eff}}(\mathbf{r})$ in a sample, then the local magnetization $\mathbf{M}(\mathbf{r})$ aligns eventually to its direction to minimize magnetic energy. The torque equation of motion of the unit vector of magnetization $\mathbf{m}(\mathbf{r},t)=\mathbf{M}(\mathbf{r},t)/M_s$ is $\dot{\mathbf{m}}=\gamma\mathbf{H}_{\text{eff}}\times\mathbf{m}$ (here M_s is the saturation magnetization, dot over the symbol means derivative with respect to time, and γ is the gyromagnetic ratio). This equation, however, describes only a precession around the field $\mathbf{H}_{\text{eff}}$ and does not account any energy dissipation. Landau and Lifshitz accounted the dissipation [1] by adding a damping torque to the equation of magnetization motion:

$$\dot{\mathbf{m}}=\gamma\mathbf{H}_{\text{eff}}\times\mathbf{m}+\gamma\alpha_{LL}\,\mathbf{m}\times(\mathbf{m}\times\mathbf{H}_{\text{eff}}), \qquad (1)$$

where the last term describes the damping torque, which tends to align $\mathbf{m}$ along $\mathbf{H}_{\text{eff}}$, and α_{LL} is a relaxation constant. Later in 1955, Gilbert [2] using a Lagrangian approach to the magnetization dynamics and Rayleigh dissipation function proposed another form of the damping, which contains $\dot{\mathbf{m}}$,

$$\dot{\mathbf{m}}=\gamma\mathbf{H}_{\text{eff}}\times\mathbf{m}+\alpha_G\,\mathbf{m}\times\dot{\mathbf{m}}, \qquad (2)$$

where $\alpha_G<<1$ is a phenomenological Gilbert damping constant [2] (e.g., for permalloy $\alpha_G\approx 0.01$). Equation (2) is called the Landau–Lifshitz–Gilbert (LLG) equation. Despite of its phenomenological origin, the LLG equation is widely used in the modern magnetism on the mesoscopic (10–100 nm) and microscopic length scales. Damping parameter α_G is usually treated as a scalar constant and is frequently determined from the line broadening in ferromagnetic resonance measurements.

Equations (1), (2) are essentially equivalent, and they describe correctly the decay of magnetization precession and relaxation to the equilibrium direction, $\mathbf{m}\,\|\,\mathbf{H}_{\text{eff}}$, for many particular cases. In the above, α_{LL} and α_G are dimensionless parameters. As it was shown (for instance, see Ref. 3), the damping terms of Gilbert form can be derived by integrating out the environment degrees of freedom. Although the LL and LLG damping terms are mathematically equivalent and give the same solutions for small damping ($\alpha_{LL}<<1$, $\alpha_G<<1$), the LLG equation repre-

sents better the relaxation behavior when the damping parameter is large [4]. We show below that there is an additional contribution to the Gilbert damping in the LLG equation in metallic ferromagnets due to spatial inhomogeneity of the moving magnetization $\mathbf{m}(\mathbf{r},t)$.

The effective magnetic field $\mathbf{H}_{\text{eff}}$ is a functional derivative of the magnetic energy, $\mathbf{H}_{\text{eff}}(\mathbf{r}) = -\delta E/\delta \mathbf{M}(\mathbf{r})$, and it includes the exchange field, the magnetic anisotropy field, external field and the nonlocal demagnetizing field. Thus, Eqs. (1), (2) are nonlinear integro-differential equations, and can be solved analytically in some limited number of simple particular cases. Nowadays powerful micromagnetic simulation codes [5] based on the LLG equation have already become a standard tool for studying the magnetization dynamics of complex magnetization distributions on timescales which are longer than 10 ps (the oscillation frequency is less than 100 GHz).

The damping term in Eq. (2) comes from different relaxation processes that do not necessarily involve conduction electrons, and thus present even in insulating ferromagnets. Since many magnetic properties such as magnetic hysteresis are not sensitive to the origin of the damping parameter, one could use this equation without paying much attention to the details of damping mechanism. However, there are other cases, where details of the damping are important. For example, the current-induced spin torque [6] directly competes with the damping torque and thus the threshold currents depend on the strength and form of the damping. The damping is usually determined by two-magnon scattering on the sample imperfections. Therefore, sometimes it is considered as an extrinsic parameter.

There is a number of the papers dedicated to the investigation of the different forms and sources of the damping in the Landau–Lifshitz equation [7–16]. It was shown [9–12] that an extension of the LLG equation is needed, but it is unclear whether accounting for other damping terms would describe the magnetization dynamics better due to complexity of many microscopic damping mechanisms. The essential contribution to understanding of the magnetization damping was done by Baryakhtar *et al*. (see Ref. 8 and references therein). Baryakhtar *et al*. suggested to include to the damping torque in the LL equation the relaxation terms of both relativistic and exchange nature and account explicitly for the symmetry of crystal lattice and spatial derivatives of the effective field. The general phenomenological approach to the magnetic relaxation was formulated in Ref. 8 and applied to relaxation of magnetic solitons in bulk magnets. The limits of applicability of the damping terms (1, 2) were established [8]. It was shown that the LL and Gilbert damping terms cannot properly describe relaxation in the magnetic systems with continuously degenerated ground state, for instance, in uniaxial “easy plane” ferromagnets [8]. Considering a semiphenomenological model of an isolated classical spin interacting with the bath modeled by stochastic Langevin fields in the whole range of temperatures has led to the closed equation of motion for magnetization interpolating between the Landau–Lifshitz and Bloch equations at low and high temperatures — the Landau–Lifshitz–Bloch (LLB) equation [7]. The spin-spin interactions responsible for ferromagnetism were taken into account within the simplest, mean field approximation. Nevertheless, both transverse and longitudinal relaxation of magnetization were naturally accounted in this approach [7].

In conducting ferromagnets, the most significant source of damping are the conduction electrons that carry away the excess angular momentum of the precessing magnetization via interband and intraband transitions [13,14]. For instance, an enhanced Gilbert damping constant was calculated on the ferromagnetic/nonmagnetic metal interface as a result of spin “pumping” from precessing magnetization in ferromagnetic layer into adjacent normal metal layer [9]. For the complex magnetization textures like magnetic vortex, it was shown in Ref. 15 that the effective phenomenological damping increases due to the inhomogeneity of magnetization structure. This damping was found to be a function of the sizes of magnetic dot, where the vortex is moving. The extension of LLG phenomenology including the spin-texture effects stemming from the dynamically generated emergent electric and magnetic fields for magnetization motion was done in Refs. 16, 17. The additional LLG damping was written via spatial derivatives of magnetization and estimated to be comparable with the bare Gilbert damping. The deeper understanding of the damping process is rather complex. In the literature there are various approaches to derive the LLG equation or extension of this equation from microscopic theories (see a recent review [18]).

In this paper, we use the *s–d* exchange model and define gauge electric and magnetic fields appearing due to transformation to the local quantization axis of magnetization determined by the strong exchange interaction. We represent the additional damping in the LLG equation coming from the conduction electrons in a form convenient for description of magnetic solitons (domain walls, vortices, skyrmions) within the collective coordinate approach. Then, we calculate this damping for the particular case of a magnetic vortex moving in a thin circular ferromagnetic nanodot.

2. General approach

Here we consider an extension of the LLG equation (2) accounting for an additional damping contribution. The second term in Eq. (2) describes the magnetization damping, i.e., the transfer of angular momentum from the spin system to other degrees of freedom, e.g., to the lattice.

2.1. The s–d exchange interaction and gauge fields

One of the simplest approaches to extend the LLG equation on the basis of a microscopic theory is the *s–d* exchange model. In this model the electrons are subdivided

into two types: (1) itinerant conduction electrons (denoted as *s* electrons) with energies close to the Fermi level ε_F, which are responsible for the spin-dependent transport, and (2) localized electrons (classical magnetization field **M**) far below ε_F (denoted as *d* electrons), which give the main contribution to $\mathbf{m}(\mathbf{r},t)$ (inducing in turn a spin polarization to the *s* electrons). These *s* and *d* electrons are treated as distinct degrees of freedom, which are coupled by the *s*–*d* exchange interaction $H_{sd} = -J\boldsymbol{\sigma}\cdot\mathbf{m}(\mathbf{r},t)$, where $\mathbf{m}(\mathbf{r},t)$ is the unit vector representing the direction of the local magnetization, $\boldsymbol{\sigma} = (\sigma_x, \sigma_y, \sigma_z)$ is the Pauli spin matrix vector for the conduction electrons, J is the exchange coupling strength. An important point is that J is rather strong in 3*d* ferromagnets, $J/\varepsilon_F \approx 0.1$ ($J \approx 1$ eV). That is why this interaction should be taken into account in the zero-approximation in the conductivity electron Hamiltonian.

The rotation of the spin coordinate system locally (a gauge transformation) was successfully used for a new formulation of Fermi-liquid theory in Ref. 19 for describing the itinerant ferromagnetism, in particular in iron, cobalt and nickel. Later, in Ref. 20 the gauge transformation was applied to derive the LL equation from the simple model of ferromagnetism in the system of localized fermions with spin 1/2. Then, by using the same approach the LLG equation was generalized in Refs. 16, 21, 22 for the systems with inhomogeneous $\mathbf{m}(\mathbf{r},t)$. The idea behind was that the magnetization produced by the conduction electrons in general is not parallel to $\mathbf{m}(\mathbf{r},t)$. As far as conduction electrons experience spin-flip scattering processes, they cannot follow $\mathbf{m}(\mathbf{r},t)$ immediately [22]. But the conduction electron time and spatial scales are much smaller than ones for the magnetization $\mathbf{m}(\mathbf{r},t)$ and we assume that the electron spins follow the variations of $\mathbf{m}(\mathbf{r},t)$ (adiabatic approximation [16,22]). Thus, a torque density is exerted on $\mathbf{m}(\mathbf{r},t)$ via the exchange interaction between the conduction and localized electrons described by the Hamiltonian H_{sd} above. This torque should be added to the LLG equation (2). The generalization of the LLG equation with the damping scalar α_G is [22]

$$\dot{\mathbf{m}} = \gamma\,\mathbf{H}_{\text{eff}}\times\mathbf{m} + \alpha_G\,\mathbf{m}\times\dot{\mathbf{m}} + \mathbf{T}. \qquad (3)$$

In order to know the extra torque $\mathbf{T}$, we should calculate the spin current generated by conduction electrons. For this purpose we describe the conduction electron states by a wavefunction ψ. This single-particle wavefunction for conduction electrons satisfies the Schrödinger equation $i\hbar\,\partial\psi/\partial t = H\psi$ with the Hamiltonian $H = p^2/(2m) + H_{sd}$. As far as the magnetization vector $\mathbf{m}(\mathbf{r},t)$ varies in space and time, one can choose the appropriate 2×2 unitary matrix $U(\mathbf{r},t) = \exp(-i\theta\boldsymbol{\sigma}\cdot\mathbf{n}/2)$ such as $U^+(\mathbf{r},t)(\mathbf{m}(\mathbf{r},t)\cdot\boldsymbol{\sigma})U(\mathbf{r},t) = \sigma_z$, where θ is the angle of rotation of the quantization axis from the fixed axis $\mathbf{e}_z$ to the axis parallel to $\mathbf{m}$ at given $(\mathbf{r},t)$ and the vector $\mathbf{n} = \mathbf{e}_z\times\mathbf{m}/|\mathbf{e}_z\times\mathbf{m}|$ represents the axis of rotation. Thus, we rotate locally the electron spin quantization axis to be parallel to the local magnetization vector $\mathbf{m}(\mathbf{r},t)$. By replacing $\psi = U\psi'$ we can diagonalize H_{sd} in the spin space and the new Schrödinger equation becomes

$$i\hbar\,\partial\psi'/\partial t = \left((\mathbf{p} - e\mathbf{A})^2/(2m) + eV + J\sigma_z\right)\psi'$$

with the spin-dependent scalar and vector potentials $V = -(i\hbar/e)U^+\partial_t U$ and $\mathbf{A} = (i\hbar/e)U^+\nabla U$ being considered as perturbations. These potentials can be projected to two spin-up and spin-down bands with respect to the local direction of $\mathbf{m}(\mathbf{r},t)$. The gauge electric and magnetic fields for each spin band can be introduced as $E_i^{\uparrow\downarrow} = -\partial_i V - \partial_t A_i$ and $B_i = (\nabla\times\mathbf{A})_i$ and may be represented in terms of $\mathbf{m}$, $\partial_t\mathbf{m}$ and $\partial_i\mathbf{m}$ ($i = x, y, z$) [16]. Since the conductivities $G^{\uparrow\downarrow}$ for spin-up and spin-down channels are different, the gauge electric field generates both electrical and spin currents. Electric current is calculated by Ohm's law for each spin channel $j_i^{\uparrow\downarrow} = G^{\uparrow\downarrow}E_i^{\uparrow\downarrow}$. The total charge and spin currents are $j_i^{\text{ch}} = j_i^{\uparrow} + j_i^{\downarrow}$ and $j_i^{\text{spin}} = j_i^{\uparrow} - j_i^{\downarrow}$. The spin current carries a spin angular momentum. If one uses continuity equation for the angular momentum, the divergence of the spin current is identified as the change of total angular momentum [16], or as spin torque $\mathbf{T}_e(\mathbf{r},t) = -\sum_i \partial_i j_i^{\text{spin}}(\mathbf{r},t)$ received from the local moving magnetization $\mathbf{m}$. The extra torque $\mathbf{T}$ acting on the magnetization is the opposite to the *s*-electrons spin torque $\mathbf{T}_e$. If we calculate the explicit expressions for the emergent electric fields $E_i^{\uparrow\downarrow}$ via derivatives of $\mathbf{m}$ and insert this extra torque to Eq. (3), then it has the form of an additional damping torque and the generalized LLG equation reads as

$$\partial_t\mathbf{m} = \gamma\,\mathbf{H}_{\text{eff}}\times\mathbf{m} + \mathbf{m}\times(\hat{D}\cdot\partial_t\mathbf{m}), \qquad (4)$$

where $D_{\alpha\beta}$ is the 3×3 damping matrix [16]:

$$D_{\alpha\beta} = \alpha_G\delta_{\alpha\beta} + \eta\sum_i(\mathbf{m}\times\partial_i\mathbf{m})_\alpha\,(\mathbf{m}\times\partial_i\mathbf{m})_\beta, \qquad (5)$$

where $\delta_{\alpha\beta}$ is the unit matrix element, $\eta = g\mu_B\hbar G_0/(4e^2M_s)$, $G_0 = G^{\uparrow} + G^{\downarrow}$ is the sum of the conductivities for the spin-up $G^{\uparrow}$ and spin-down $G^{\downarrow}$ bands. We notice that the enhanced damping parameter η is proportional to the material conductivity. This is not surprising because the larger the conductivity, the more rapidly the angular momenta are carried away by the conduction electrons. Thus, the LLG equation with the damping given by Eq. (5) is more significant for magnetic materials with large conductivities. Estimation of the magnitude of η can be readily done for transition 3*d*

metals. For example, if we use $G_0 = (5\mu\Omega\cdot\text{cm})^{-1}$ and $M_s = 800$ emu/cc for permalloy (NiFe alloy), we find that $\eta = 0.5$ nm^2.

2.2. The magnetization damping of dynamical spin texture

By using the relation $\mathbf{H}_{\text{eff}} = -M_s^{-1}\partial E/\partial\mathbf{m}$ the equation of motion Eq. (4) can be rewritten in the following way:

$$\partial_t\mathbf{m} = \mathbf{m}\times\left[\frac{\gamma}{M_s}\frac{\partial E}{\partial\mathbf{m}} + (\hat{D}\,\partial_t\mathbf{m})\right], \tag{6}$$

where E is the total magnetic energy density. As far as E in Eq. (6) includes local (e.g., the exchange, Zeeman and anisotropy energies) as well as the dipolar nonlocal long-range interactions, Eq. (6) is a nonlinear and nonlocal equation with multiple length and time scales solvable in only a few simple cases. For example, in the case of translational motion of a spin texture (domain wall, vortex, skyrmion), $\mathbf{m} = \mathbf{m}[\mathbf{r},\mathbf{s}(t)]$, the LLG equation can be fully parameterized by the texture's "enter-of-mass" collective coordinate $\mathbf{s}$. Such parameterization is very useful to simplify Eq. (6) because we can write $\partial_t\mathbf{m} = (\partial\mathbf{m}/\partial s_\beta)\partial_t s_\beta$. If we calculate the vector product of $\partial\mathbf{m}/\partial s_\alpha$ and Eq. (6), and then multiply this product by $\mathbf{m}$, we get

$$\mathbf{m}\cdot\left(\frac{\partial\mathbf{m}}{\partial s_\alpha}\times\frac{\partial\mathbf{m}}{\partial s_\beta}\right)\partial_t s_\beta = \frac{\gamma}{M_s}\frac{\partial E}{\partial s_\alpha} + \hat{D}\left(\frac{\partial\mathbf{m}}{\partial s_\beta}\partial_t s_\beta\right)\frac{\partial\mathbf{m}}{\partial s_\alpha}. \tag{7}$$

The last product in Eq. (7) is equal to $\sum_{\gamma\gamma'} D_{\gamma\gamma'}\,\partial_t s_\beta(\partial m_\gamma/\partial s_\alpha)(\partial m_{\gamma'}/\partial s_\beta)$. After the integration of Eq. (7) over the whole volume of the magnetic material (it is a magnetic cylindrical nanodot in the case considered below), we get the Thiele equation of motion [23] for the center of magnetization texture $\mathbf{s} = (s_x, s_y)$:

$$G_{\alpha\beta}\,\partial_t s_\beta = F_\alpha + \Gamma_{\alpha\beta}\,\partial_t s_\beta. \tag{8}$$

The differential Thiele equation (8) is a simplified form of the LLG equation and sometimes it can be solved analytically. In this equation $G_{\alpha\beta}$ is an anti-symmetric gyrotropic tensor, F_α is the net conservative force, and $\Gamma_{\alpha\beta}$ is a dissipation tensor:

$$G_{\alpha\beta} = \frac{M_s}{\gamma}\int dV\,\mathbf{m}\cdot\frac{\partial\mathbf{m}}{\partial s_\alpha}\times\frac{\partial\mathbf{m}}{\partial s_\beta}, \tag{9}$$

$$F_\alpha = -\int dV\,\frac{\delta E}{\delta\mathbf{m}}\cdot\frac{\partial\mathbf{m}}{\partial s_\alpha}, \tag{10}$$

$$\Gamma_{\alpha\beta} = \frac{M_s}{\gamma}\int dV\sum_{\gamma\gamma'} D_{\gamma\gamma'}\frac{\partial m_\gamma}{\partial s_\alpha}\frac{\partial m_{\gamma'}}{\partial s_\beta}. \tag{11}$$

A magnetization texture moves like a massless particle with electric charge in an effective magnetic field determined by the gyrotropic tensor (9) and an external potential (10) through a viscous medium. Although Eq. (8) was derived by Thiele for the steady state motion of magnetic domain walls in bulk magnets, this equation using definitions given by Eqs. (9)–(11) can serve as a good approximation in more general situations. The Thiele equation is widely used for describing the domain wall and vortex/skyrmion dynamics in magnetic dots, stripes etc. In the present paper we calculate the damping tensor $\Gamma_{\alpha\beta}$ (11) taking into account the conduction electrons. By using Eq. (5), we can rewrite Eq. (11) in the following form:

$$\Gamma_{\alpha\beta} = \frac{M_s}{\gamma}\times$$

$$\times\int dV\left[\alpha_G\frac{\partial\mathbf{m}}{\partial s_\alpha}\cdot\frac{\partial\mathbf{m}}{\partial s_\beta} + \eta\mathbf{m}\cdot\left(\frac{\partial\mathbf{m}}{\partial x_i}\times\frac{\partial\mathbf{m}}{\partial s_\alpha}\right)\mathbf{m}\cdot\left(\frac{\partial\mathbf{m}}{\partial x_i}\times\frac{\partial\mathbf{m}}{\partial s_\beta}\right)\right]. \tag{12}$$

The first term in Eq. (12) is proportional to the phenomenological Gilbert damping α_G that comes from all the sources in the material except the mechanism of *s–d* interaction considered here. The second term represents the influence of the conduction electrons. It is shown in Ref. 16 that the η-term corresponds to the magnetization dissipation rate equal to the Joule heating rate in the emergent electric fields $\mathbf{E}^{\uparrow\downarrow}$. One can notice from Eq. (8) that the diagonal elements $\Gamma_{\alpha\alpha}$ represent the actual damping and the nondiagonal $\Gamma_{\alpha\beta}$ elements renormalize the gyrotensor, which has no diagonal components. Thus, here we are interested in the diagonal elements of the damping tensor:

$$\Gamma_{\alpha\alpha} = \frac{M_s}{\gamma}\int dV\left[\alpha_G\left(\frac{\partial\mathbf{m}}{\partial s_\alpha}\right)^2 + \eta\left(\mathbf{m}\cdot\left(\frac{\partial\mathbf{m}}{\partial x_i}\times\frac{\partial\mathbf{m}}{\partial s_\alpha}\right)\right)^2\right]. \tag{13}$$

The unit vector of magnetization can be defined by the spherical angles Θ, Φ as

$$\mathbf{m} = (\sin\Theta\cos\Phi,\ \sin\Theta\sin\Phi,\ \cos\Theta).$$

For simplicity we rewrite the damping tensor as the sum of phenomenological contribution and an additional damping related to the conduction electrons $\Gamma_{\alpha\alpha} = \Gamma_\alpha^{\text{ph}} + \Gamma_\alpha^{\text{add}}$. In order to simplify Eq. (13) we use a relation between the gauge field vector-potential $A_\mu = (A_0, \mathbf{A})$, $A_\mu = (i\hbar/e)U^+\partial_\mu U$ $(\partial_\mu = (\partial/\partial t, \nabla))$ and the magnetization vector $\partial_\mu\mathbf{m}\times\partial_\nu\mathbf{m} = 4\mathbf{m}(A_\mu^\theta A_\nu^\varphi - A_\nu^\theta A_\mu^\varphi)$ taken from the paper by Tatara *et al.* [24], Eq. (160), where the components of the gauge potential are defined as $A_\mu^\theta \equiv -(1/2)\sin\Theta\,\partial_\mu\Phi$ and $A_\mu^\varphi \equiv (1/2)\,\partial_\mu\Theta$. Using the relation $\partial_t\mathbf{m} = (\partial\mathbf{m}/\partial s_\beta)\,\partial_t s_\beta$, we get for the diagonal components of the damping tensor:

$$\Gamma_\alpha^{\rm ph} = \frac{M_s}{\gamma}\alpha_G \int dV \left[\left(\frac{\partial \Theta}{\partial s_\alpha} \right)^2 + \sin^2 \Theta \left(\frac{\partial \Phi}{\partial s_\alpha} \right)^2 \right], \quad (14)$$

$$\Gamma_\alpha^{\rm add} = \frac{M_s}{\gamma}\eta \int dV \, \sin^2 \Theta \left[\nabla\Theta \frac{\partial \Phi}{\partial s_\alpha} - \nabla\Phi \frac{\partial \Theta}{\partial s_\alpha} \right]^2. \quad (15)$$

Equations (14), (15) are written in general form for any moving inhomogeneous magnetization configuration in the form $\mathbf{m} = \mathbf{m}[\mathbf{r}, \mathbf{s}(t)]$, where $\mathbf{s}(t)$ is a spin texture (soliton) center position. In the next section we apply these equations to moving magnetic vortex in a nanodot. In particular, we are interested in calculation of $\Gamma_\alpha^{\rm add}$ for the vortex magnetization configuration.

3. Damping of moving magnetic vortex

Here we consider a magnetic vortex in cylindrical nanodot of thickness L and radius R (Fig. 1). The static vortex is the dot ground state for a wide range of L and R [15]. The typical nanodot is thin (thickness L is about of 10–30 nm) and the dependence of the vortex configuration on the dot thickness can be neglected. Then, we can integrate Eqs. (14), (15) over the dot thickness. We can safely use the Gilbert damping in Eqs. (6) and (8) because the system relaxes to the nondegenerate ground state $\mathbf{s} = 0$. The phenomenological damping $\Gamma_\alpha^{\rm ph}$ for magnetic vortex moving in a circular nanodot has already been calculated in Ref. 15 as $\Gamma_\alpha^{\rm ph} = \alpha_G 2\pi M_s L[b + \ln(R/R_c)/2]/\gamma$, where $R_c(L)/l_{\rm ex} = 0.59 + 0.21(L/l_{\rm ex})^{0.85}$ [25] is the thickness dependent vortex core radius, $l_{\rm ex} = \sqrt{2A}/M_s$, and A is the material exchange stiffness. The parameter b is $b = 1$ within the rigid vortex model [25] or $b = 5/8$ within two-vortex model [26]. Thus, the phenomenological damping is a function of the dot geometrical parameters (R and L).

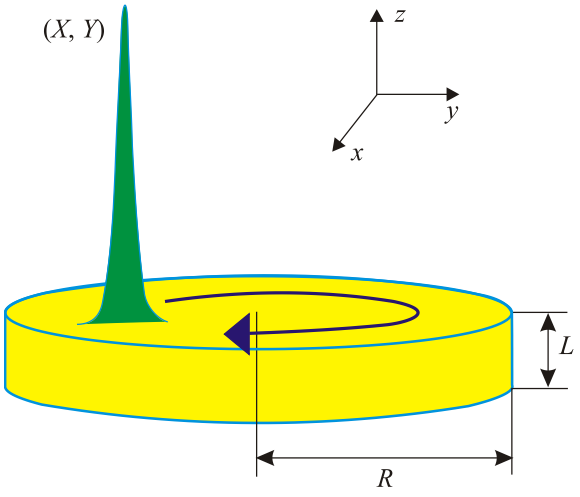

Fig. 1. Magnetic vortex in cylindrical nanodot with radius R and thickness L. The vortex core position is $\mathbf{X} = (X,Y)$. The dimensionless core displacement is $\mathbf{s} = \mathbf{X}/R$.

Concerning the additional damping, after the integration over the dot thickness we get $\Gamma_\alpha^{\rm add} = \eta M_s L I_\alpha/\gamma R^2$, where $I_\alpha = \int d^2\boldsymbol{\rho} \sin^2 \Theta[\nabla\Theta(\partial\Phi/\partial s_\alpha) - \nabla\Phi(\partial\Theta/\partial s_\alpha)]^2$ and the integration coordinates and the vector $\mathbf{s}$ are normalized to the dot radius R. This damping can be significant due to a complex magnetization distribution of the vortex state. The dynamical vortex profile in the linear approximation on small core displacement $\mathbf{X}$ ($\mathbf{s} = \mathbf{X}/R$, $|\mathbf{s}| << 1$) from equilibrium position in the dot center can be written within two-vortex model accounting absence of the dot side surface magnetic charges [26,27] as $m_z(\boldsymbol{\rho}, \mathbf{s}) = \cos\Theta = m_z^0(\rho) + g(\rho)(\mathbf{s}\cdot\hat{\boldsymbol{\rho}})$ and $\Phi(\boldsymbol{\rho}, \mathbf{s}) = C\pi/2 + \varphi + m_0(\rho)[s_x \sin\varphi - s_y \cos\varphi]$, where $m_0(\rho) = (1-\rho^2)/\rho$ is the gyrotropic mode profile, $g(\rho) = 4pc^2\rho(1+\rho^2)/(c^2+\rho^2)^2$, $p = m_z(0) = \pm 1$ is the vortex core polarization, $C = \pm 1$ is the vortex chirality, and $\boldsymbol{\rho} = (\rho, \varphi)$ is the polar radius-vector. Thus, we can rewrite the integral I_α in the following form:

$$I_\alpha = \int\limits_{\rm core} d^2\boldsymbol{\rho} \left(\frac{\partial \Phi}{\partial s_\alpha} \nabla m_z - \frac{\partial m_z}{\partial s_\alpha} \nabla\Phi \right)^2. \quad (16)$$

The damping $\Gamma_\alpha^{\rm add} \propto I_\alpha$ is solely determined by the vortex core because $m_z = 0$ (negligibly small) outside the vortex core by definition. One can show that $\nabla m_z = \mathbf{e}_\rho p(-4\rho c^2)/(c^2+\rho^2)^2$. The profile of z-component of magnetization inside the vortex core is $m_z = (1-|f|^2)/(1+|f|^2)$, where

$$f = -(i/c)(z-s)(z\bar{s}-1)/(1+|s|^2)$$

within two-vortex model [26], $c = R_c/R$ is the dimensionless vortex core radius, $s = s_x + is_y$, and $z = x + iy$. Our calculations show that

$$\partial m_z/\partial s_x = -4c^2\rho\cos\varphi(1+\rho^2)/(c^2+\rho^2)^2, \quad s \to 0.$$

After all the substitutions to Eq. (16) and integration over the vortex core region we get within the limit of linear dynamics determined by Eq. (8), $s \to 0$, the integrals I_α

$$I = I_x = I_y = \frac{2\pi}{3c^2}(7 + c^4). \quad (17)$$

For analytical integration we used the equations (2.115.1-3) from Ref. 28. The additional damping is $\Gamma^{\rm add} = \Gamma_{x,y}^{\rm add} = \eta M_s L I(c)/(\gamma R^2)$. Usually, the vortex core radius is small comparing with the dot radius $c \approx 0.10$, thus from Eq. (17) we get $I(c) \approx 14\pi/(3c^2)$. Then, the additional damping can be expressed in the form

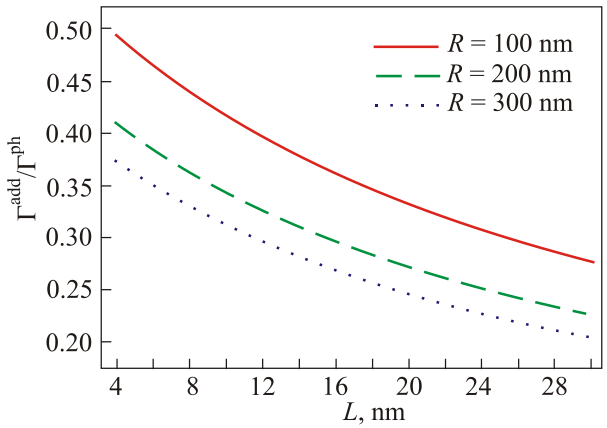

Fig. 2. The ratio of additional damping Γ^{add} due to the conduction electrons and phenomenological Gilbert damping Γ^{ph} calculated by Eq. (19) for a circular permalloy dot using the explicit dependence of the vortex core radius on the dot thickness, $R_c(L)$.

$$\Gamma^{add} = \frac{7}{3} G (R_\eta / R_c)^2, \tag{18}$$

where $G = 2\pi M_s L/\gamma$ is the magnitude of gyrovector $\mathbf{G} = G\mathbf{z}$ calculated as $G = G_{xy}$ using Eq. (9), $R_\eta = \sqrt{\eta}$ $R_\eta = 0.7$ nm for permalloy), and $R_c \approx 10$ nm. We see that the damping Γ^{add} (18) is determined by the small ratio $(R_\eta/R_c)^2$. The ratio of the additional damping Γ_α^{add} to the phenomenological Gilbert damping Γ^{ph} can be written in the following form:

$$\frac{\Gamma^{add}}{\Gamma^{ph}} = \frac{1}{2\pi\alpha_G} \frac{\eta}{R^2} \frac{I(R_c/R)}{b + \ln(R/R_c)/2}, \tag{19}$$

The ratio $\Gamma^{add}/\Gamma^{ph} \propto R_c^{-2}(L)[b + \ln(R/R_c(L))]^{-1}$ as a function of the dot sizes L, R is shown in Fig. 2 for typical values of L, R.

4. Discussion

It is important that the additional damping described by Eqs. (15), (18) and (19) originates from the emergent electrical fields $\mathbf{E}^{\uparrow\downarrow} = -\nabla V - \partial_t \mathbf{A}$ induced by a spatially inhomogeneous moving magnetization $\mathbf{m}(\mathbf{r},t)$, and the spatial derivatives $\partial_i \mathbf{m}(\mathbf{r},t)$ must be not equal to zero. The damping tensor has been approximated to be a constant in most studies [26,27,29,30] on magnetic vortex dynamics assuming that the vortex core is positioned near the dot center. However, in the recent paper [31] it was shown by micromagnetic modeling that the gyrovector and damping parameters are changing with the vortex oscillations. We showed that the ratio Γ^{add}/Γ^{ph} varies from 0.2 to 0.5 for permalloy ($Ni_{80}Fe_{20}$ alloy) and typical dot sizes (Fig. 2). I.e., the additional damping is approximately equal to 40% of the phenomenological damping. For other ferromagnetic metals and alloys with lower bare Gilbert damping α_G and/or higher conductivity, the ratio Γ^{add}/Γ^{ph} can be different and might by order of unit. The same approach to the additional magnetic vortex damping has been used in [32], where the micromagnetic simulations with and without additional damping in the form of $D_{\alpha\beta}$ given by Eq. (5) were performed. In the present paper we have written the damping term in a convenient form for analytical calculations. Equations (14), (15) are general and can be used for any magnetization distribution if the soliton profiles Θ, Φ are known. Then, the damping tensor $\Gamma_{\alpha\beta}$ can be calculated in the main approximation $\Gamma_{\alpha\beta}(\mathbf{s}=0)$ for the soliton equilibrium position $\mathbf{s} = 0$.

It was found in Ref. 32 that the enhanced damping does not change the frequency of vortex gyrotropic oscillations, while the gyration radius and velocity of a vortex core decrease when considering the total damping tensor (12). In the present paper we calculated analytically the additional damping for small vortex core displacements $|\mathbf{s}| << 1$. However, our calculations would be extended for larger vortex core displacements beyond the linear approximation [30]. We assume that there should be an enhancement of the additional damping and a decrease of the vortex gyration radius in the nonlinear regime.

In principle, the additional magnetization damping should be taken into account for magnetic nanodots made of ferromagnetic metals (Co, FeNi) with small thicknesses (5–10 nm), which normally are used as a free layer in the spin-torque nanooscillators (STNO). However, it is difficult from the experimental point of view to detect such contribution to the magnetization damping. For our dot parameters and room temperature the ratio $\Gamma_\alpha^{add}/\Gamma^{ph}$ does not exceed 1, which means that the additional damping does not play a dominant role (at least in the considered linear regime of the vortex motion). Up to now there are no direct experimental measurements of the damping influence on the vortex or skyrmion dynamics. The electro-motive force acting on the moving vortex and explained by the equation for an emergent electric field $E_i^{\uparrow\downarrow} = -\partial_i V - \partial_t A_i$ should be large enough to be measured experimentally as reported in Ref. 33, where an experimental scheme of its detection was proposed. However, the sole additional damping may be not easy to measure. Taking into account Fig. 2 and Ref. 32 we can propose some experimental way to detect this additional damping. In a dynamical experiment it should be easy either change temperature or external magnetic field. In our calculations we did not take into account the temperature dependence of the conductivity G_0 that is beyond our calculations. In Ref. 34 (see Fig. 5) such dependences were measured experimentally for permalloy (Py) and it was shown, that if temperature is decreased from room temperature to 4 K, the conductivity of Py can increase for approximately 20%.

As far as $\Gamma_\alpha^{\text{add}}$ is proportional to conductivity, then it would also increase with the temperature decreasing (the dependence $M_s(T)$ is approximately constant if $T << T_c$, T_c(Py) ≈ 700 K). The external perpendicular magnetic field would also change the additional damping. If the magnetic bias field is applied in the direction opposite to the vortex core polarization, then the size of vortex core R_c is shrinking. As far as $\Gamma_\alpha^{\text{add}} \propto 1/R_c^2$, then additional damping can increase a lot, if we are talking about small displacements of the vortex core from its equilibrium position. $\Gamma_\alpha^{\text{add}}$ would also be important for large vortex core displacement applying in-plane bias field, when the region of magnetization inhomogeneity increases with the modification of the vortex core. The detected ferromagnetic resonance linewidth increased in ≈ 2 times in permalloy nanodots [35] approaching the vortex state decreasing the applied in-plane field from the vortex annihilation field to the vortex nucleation field. Accounting that the vortex nucleation means appearance of nonzero m_z magnetization component and nonzero integral over the forming vortex core presented by Eq. (16), the observed effect of the considerable ferromagnetic resonance linewidth increase [35] could be a result of the additional damping increase.

Conclusions

In the present paper we considered the extended Landau–Lifshitz–Gilbert (LLG) equation of magnetization motion for the case of conducting ferromagnet with an inhomogeneous magnetization texture and showed that an additional damping appears due to spin currents generated by emergent electric fields, which are determined by the spatial and time derivatives of the magnetization. We represented the additional damping in the LLG equation coming from the conduction electrons in a form convenient for description of magnetic solitons (domain walls, vortices, skyrmions) within the collective coordinate approach. We calculated this additional damping for the particular case of the moving vortex in a circular nanodot. It is shown that this additional damping depends on the dot sizes and can reach up to 50% of the phenomenological Gilbert damping. It should be taken into account for interpretation of the spin torque vortex oscillator dynamics and ferromagnetic resonance measurements of spatially inhomogeneous magnetization textures. This additional damping can also be significant for description of the vortex domain wall and skyrmion dynamics.

Acknowledgments

K.G. acknowledges support by IKERBASQUE (the Basque Foundation for Science). O.S. acknowledges financial support by the University of the Basque Country, UPV/EHU. This work was partially supported by the Spanish Ministerio de Economia y Competitividad under the grant MAT2013-47078-C2-1-P.

1. L.D. Landau and E.M. Lifshitz, *Phys. Z. Sowejetunion* **8**, 153 (1935).
2. T.L. Gilbert, *Phys. Rev*. **100**, 1243 (1955); see also T.L. Gilbert, *IEEE Trans. Magn*. **40**, 3443 (2004).
3. G. Tatara, H. Kohno, and J. Shibata, *J. Phys. Soc. Jpn*. **77**, 031003 (2008).
4. T.L. Gilbert and J.M. Kelly, *Conf. Magn. Magn. Mater*., Pittsburgh, PA, June 14–16, 1955, New York: American Inst. of Electrical Engineers, Oct. (1955), p. 253.
5. See, for instance, http://math.nist.gov/oommf
6. J. Slonczewski, *J. Magn. Magn. Mater*. **159**, L1 (1996).
7. D.A. Garanin, *Phys. Rev. B* **55**, 3050 (1997).
8. V.G. Baryakhtar, B.A. Ivanov, A.L. Sukstanskii, and E.Yu. Melikhov, *Phys. Rev. B* **56**, 619 (1997); V.G. Baryakhtar and A.G. Danilevich, *Fiz. Nizk. Temp*. **39**, 1279 (2013) [*Low Temp. Phys.* **39**, 993 (2013)].
9. Y. Tserkovnyak, A. Brataas, and G.E.W. Bauer, *Phys. Rev. Lett.* **88**, 117601 (2002).
10. E. Rossi, O.G. Heinonen, and A.H. MacDonald, *Phys. Rev. B* **72**, 174412 (2005).
11. N. Smith, *J. Appl. Phys*. **90**, 5768 (2001).
12. V.L. Safonov and H.N. Bertram, *J. Appl. Phys*. **94**, 529 (2003).
13. J. Kunes and V. Kambersky, *Phys. Rev. B* **65**, 212411 (2002).
14. K. Gilmore, Y.U. Idzerda, and M.D. Stiles, *Phys. Rev. Lett*. **99**, 027204 (2007).
15. K.Y. Guslienko, *Appl. Phys. Lett.* **89**, 022510 (2006).
16. S. Zhang and S.S.-L. Zhang, *Phys. Rev. Lett*. **102**, 086601 (2009); *IEEE Trans. Magn*. **46**, 2297 (2010).
17. C.H. Wong and Y. Tserkovnyak, *Phys. Rev. B* **81**, 060404(R) (2010).
18. M. Fähnle and C. Illg, *J. Phys.: Condens. Matter* **23**, 493201 (2011).
19. V. Korenman, J.L. Murray, and R.E. Prange, *Phys. Rev. B* **16**, 4032 (1977); *ibid.* **16**, 4058 (1977); V. Korenman and R.E. Prange, *J. Appl. Phys.* **50**, 1779 (1979).
20. G.E. Volovik, *J. Phys. C* **20**, L83 (1987).
21. L. De Angeli, D. Steiauf, R. Singer, I. Koeberle, F. Dietermann, and M. Fähnle, *Phys. Rev. B* **79**, 052406 (2009).
22. S. Zhang and Z. Li, *Phys. Rev. Lett*. **102**, 086601 (2004).
23. A.A. Thiele, *Phys. Rev. Lett*. **30**, 230 (1973).
24. G. Tatara, H. Kohno, and J. Shibata, *Phys. Rep*. **468**, 213 (2008).
25. O.V. Sukhostavets, G.R. Aranda, and K.Y. Guslienko, *J. Appl. Phys*. **111**, 093901 (2012).
26. K.Y. Guslienko, G.R. Aranda, and J. Gonzalez, *J. Phys.: Conf. Ser*. **292**, 012006 (2011).
27. K.Y. Guslienko, *J. Spintronics and Magn. Nanomater*. **1**, 70 (2012).
28. I.S. Gradshteyn and I.M. Ryzhik, *Table of Integrals, Series and Products*, 7th ed., Academic Press, New York (2007).
29. K.-S. Lee and S.-K. Kim, *Appl. Phys. Lett*. **91**, 132511 (2007).
30. K.Y. Guslienko, R.H. Heredero, and O. Chubykalo-Fesenko, *Phys. Rev. B* **82**, 014402 (2010).

31. J.-H. Shim, H.-G. Piao, S.H. Lee, S.K. Oh, S.-C. Yu, S. K. Han, and D.-H. Kim, *Appl. Phys. Lett.* **99**, 142505 (2011).
32. J.-H. Moon and K.-J. Lee, *J. Appl. Phys*. **111**, 07D120 (2012).
33. J. Ohe and S. Maekawa, *J. Appl. Phys*. **105**, 07C706 (2009).
34. E. Villamor, M. Isasa, L.E. Hueso, and F. Casanova, *Phys. Rev. B* **88**, 184411 (2013).
35. K.Y. Guslienko, G.N. Kakazei, Yu.V. Kobljanskyj, G.A. Melkov, V. Novosad, and A.N. Slavin, *New J. Phys*. **16**, 063044 (2014).